On Two-Dimensional Laminar Hydromagnetic Fluid-Particle Flow Over a Surface in the Presence of a Gravity Field

Ali J. Chamkha
Department of Mechanical and Industrial Engineering,
Kuwait University,
P.O. Box 5969,
Safat, 13060, Kuwait

A continuum two-phase fluid-particle model accounting for particle-phase stresses and a body force due to the presence of a magnetic field is developed and applied to the problem of two-dimensional laminar hydromagnetic flow of a particulate suspension over a horizontal surface in the presence of a gravity field. Analytical solutions for the velocity distributions and the skin-friction coefficients of both phases are reported. Two cases of wall hydrodynamic (velocity) conditions corresponding to stationary and oscillatory velocity distributions are considered. Numerical evaluations of the analytical solutions are performed and the results are reported graphically to elucidate special features of the solutions. The effects of the particle-phase stresses and the magnetic field are illustrated through representative results for the horizontal velocity profiles, fluid-phase displacement thickness, and the complete skin-friction coefficient for various combinations of the physical parameters. It is found that the presence of the magnetic field increases the fluid-phase skin-friction coefficient for various particulate volume fraction levels while the presence of the particle-phase viscous stresses reduces it for various particle-to-fluid density ratios. [DOI: 10.1115/1.1343460]

Introduction

Deposition of solid particles from flowing fluid/solid suspensions on surfaces is an important process in various natural and engineering applications. Some possible applications include deep-bed and membrane filtration, separation of proteins, viruses, antibodies, and vaccines, atmospheric pollution, and microbial and cell transport in living systems (Yiantsios and Karabelas [1]). There have been considerable research work done on particulate deposition in laminar flows such as the reviews by Jia and Williams [2] and van de Ven [3]. Sedimentation effects for particle sizes close to one micron or larger are reported by Yao et al. [4]. Adamczyk and van de Ven [5,6] have considered particulate deposition in rectilinear flows over flat surfaces. Marmur and Ruckenstein [7] have reported on the process of cells deposition on a flat plate. Apazidis [8,9] has analyzed the velocity and temperature distributions of two-dimensional laminar flows of a particulate suspension in the presence of a gravity field. More recently, Dahlkid [10] has considered the motion of Brownian particles and sediment on an inclined plate. This work was done in relation to the process of separation of proteins, viruses, antibodies, and vaccines. Yiantsios and Karabelas [1] has studied the effect of gravity on the deposition of micron-sized particles on smooth surfaces. Their work was focused on particulate deposition from liquid suspensions with the main motivation being fouling of heat transfer or filtration equipment by suspended particles.

In many fluid-particle flows, the fluid phase may be electrically conducting and the particle-phase concentration may be high. In an environment where a magnetic field is present, these effects play an important role in altering the flow characteristics. Particle-phase viscosity effects in particulate suspensions are especially important in multiphase systems consisting of high solid particulate concentration in liquids and gases. Particle-phase viscosity is needed to model particle-particle interaction. It can be thought of as arising naturally from the averaging processes used to derive continuum equations describing either a system exhibiting turbulent fluctuations (see, for instance, Chen and Wood [11]) or a system containing discrete elements (see, for instance, Drew and Segal [12]). Also, it is often employed to facilitate numerical solutions. Particle-phase viscous effects have been investigated previously by many investigators (see, for instance, Gidaspow [13], Tsuo and Gidaspow [14], and Gadiraju et al., [15]).

In the present work, a simple two-phase model is employed in which the suspension is assumed to be somewhat dense in the sense that inter-particle collision exists and that this is accounted for by endowing the particle phase by an artificial viscosity. The fluid phase is considered to be Newtonian and electrically conducting but the particles and the surface are assumed to be electrically nonconducting and that the magnetic Reynolds number is assumed to be small. The particle phase is assumed to have uniform density distribution and is made of spherical particles having one size. The present work is a direct generalization of the work reported by Apazidis [8] on the flow characteristics of particle-fluid flow past a horizontal plate in the presence of a gravity field.

Governing Equations

Consider unsteady laminar hydromagnetic flow of a two-phase particulate suspension over a horizontal infinite surface in the presence of a gravity field. The surface is coincident with the half plane $y=0$, $x\geqslant 0$ and the flow above the surface is a uniform stream in the x-direction parallel to the surface with both phases being in equilibrium. A magnetic field with uniform strength is applied in the y-direction normal to the flow direction. Owing to the density difference between both the fluid and particle phases, a separational motion in which heavy particles falling from the flow form a layer of dense sediment on the surface while the continuous fluid phase moves in the opposite upward direction is introduced. This settling process has been called sedimentation (Wallis [16]). According to Kynch [17] and later by Apazidis [8], the vertical sedimentation of solid particles may proceed in three different ways depending on the shape of the curve of the total particle flow rate versus the volume fraction of particles in the

Contributed by the Fluids Engineering Division for publication in the JOURNAL OF FLUIDS ENGINEERING. Manuscript received by the Fluids Engineering Division November 4, 1999; revised manuscript received November 27, 2000. Associate Editor: J. Eaton.

suspension. Apazidis [8] has considered the case when a direct shock from the initial value of the particulate volume fraction α to the final fully settled value α_M is formed at the interface of the mixture and the settled particles with maximum packing existing at the surface. The fluid phase is assumed to be Newtonian and electrically conducting while the particle phase and the surface are assumed to be electrically nonconducting. The particle phase is assumed to be somewhat dense so that particle-phase stresses are considered important and is made up of spherical solid particles having one size and with a uniform density distribution. The particle Reynolds number is assumed to be less than unity so that the force interaction between the phases is limited to the linear Stokes drag force. Also, the magnetic Reynolds number is assumed to be small so that the induced magnetic field is neglected. In addition, no electric field is assumed to exist and the Hall effect is neglected. The assumption of small magnetic Reynolds number uncouples the flow equations from Maxwell's equations (see, Cramer and Pai [18]). Based on the above assumptions and treating the particle phase as a continuum (Marble [19]), the governing equations for this investigation can be written as

$$-\frac{\partial\alpha}{\partial t}+\frac{\partial}{\partial y}((1-\alpha)v)=0 \tag{1}$$

$$(1-\alpha)\rho\left(\frac{\partial u}{\partial t}+v\frac{\partial u}{\partial y}\right)=(1-\alpha)\mu\frac{\partial^2 u}{\partial y^2}-\frac{9}{2}f(\alpha)\frac{\mu}{a^2}(u-u_p)-(1-\alpha)\sigma B_0^2(u-u_\infty) \tag{2}$$

$$(1-\alpha)\rho\left(\frac{\partial v}{\partial t}+v\frac{\partial v}{\partial y}\right)=(1-\alpha)\left(\mu\frac{\partial^2 v}{\partial y^2}-\frac{\partial p}{\partial y}-\rho g\right)-\frac{9}{2}f(\alpha)\frac{\mu}{a^2}(v-v_p) \tag{3}$$

for the fluid phase and

$$\frac{\partial\alpha}{\partial t}+\frac{\partial}{\partial y}(\alpha v_p)=0 \tag{4}$$

$$\alpha\rho_p\left(\frac{\partial u_p}{\partial t}+v_p\frac{\partial u_p}{\partial y}\right)=\alpha\mu_p\frac{\partial^2 u_p}{\partial y^2}+\frac{9}{2}f(\alpha)\frac{\mu}{a^2}(u-u_p) \tag{5}$$

$$\alpha\rho_p\left(\frac{\partial v_p}{\partial t}+v_p\frac{\partial v_p}{\partial y}\right)=\alpha\left(\mu_p\frac{\partial^2 v_p}{\partial y^2}-\frac{\partial p}{\partial y}-\rho_p g\right)+\frac{9}{2}f(\alpha)\frac{\mu}{a^2}(v-v_p) \tag{6}$$

for the particle phase where t is time and y is the vertical distance; u, v, and p are the fluid-phase x-component of velocity, y-component of velocity, and pressure, respectively; α, ρ, μ, and σ are the volume fraction of particles and the fluid-phase density, dynamic viscosity, and electrical conductivity, respectively; a, g, B_0, and u_∞ are the particle radius, gravitational acceleration, magnetic induction and the free stream velocity, respectively. A subscript p indicates a property associated with the particle phase.

Equations (1)–(6) are supplemented by the function $f(\alpha)$ which is reported by Tam [20] and employed later by Apazidis [8] such that

$$f(\alpha)=\frac{\alpha(4+3(8\alpha-3\alpha^2)^{1/2}+3\alpha)}{(2-3\alpha)^2} \tag{7}$$

It is worth noting that $f(\alpha)$ represents a correction factor for the Stokes drag force on a single spherical particle and accounts for finite volume fraction of the particle phase.

For convenience, the following equations

$$\eta=\frac{y}{a},\quad \tau=\frac{ga\gamma}{\nu}t,\quad u=\frac{ga^2\gamma}{\nu}U,\quad u_p=\frac{ga^2\gamma}{\nu}U_p$$
$$v=\frac{ga^2\gamma}{\nu}V,\quad v_p=\frac{ga^2\gamma}{\nu}V_p,\quad p=-\rho g y(1-\gamma P) \tag{8}$$

are substituted into Eqs. (1)–(6) to yield

$$-\frac{\partial\alpha}{\partial\tau}+\frac{\partial}{\partial\eta}((1-\alpha)V)=0 \tag{9}$$

$$\mathrm{Re}\left(\frac{\partial U}{\partial\tau}+V\frac{\partial U}{\partial\eta}\right)=\frac{\partial^2 U}{\partial\eta^2}-\frac{9}{2}\frac{f(\alpha)}{(1-\alpha)}(U-U_p)-M^2(U-U_\infty) \tag{10}$$

$$\mathrm{Re}\left(\frac{\partial V}{\partial\tau}+V\frac{\partial V}{\partial\eta}\right)=\frac{\partial^2 V}{\partial\eta^2}+P-\frac{9}{2}\frac{f(\alpha)}{(1-\alpha)}(V-V_p) \tag{11}$$

$$\frac{\partial\alpha}{\partial\tau}+\frac{\partial}{\partial\eta}(\alpha V_p)=0 \tag{12}$$

$$\gamma\,\mathrm{Re}\left(\frac{\partial U_p}{\partial\tau}+V_p\frac{\partial U_p}{\partial\eta}\right)=\beta\frac{\partial^2 U_p}{\partial\eta^2}+\frac{9}{2}\frac{f(\alpha)}{\alpha}(U-U_p) \tag{13}$$

$$\gamma\,\mathrm{Re}\left(\frac{\partial V_p}{\partial\tau}+V_p\frac{\partial V_p}{\partial\eta}\right)=\beta\frac{\partial^2 V_p}{\partial\eta^2}+P-1+\frac{9}{2}\frac{f(\alpha)}{\alpha}(V-V_p) \tag{14}$$

where

$$\gamma=\frac{\rho_p}{\rho},\quad \mathrm{Re}=\frac{ga^3\gamma}{\nu^2},\quad \nu=\frac{\mu}{\rho},\quad M^2=\frac{\sigma B_0^2 a^2}{\mu},$$
$$U_\infty=\frac{u_\infty\nu}{ga^2\gamma},\quad \beta=\frac{\mu_p}{\mu} \tag{15}$$

are the particle-to-fluid density ratio, Reynolds number based on the particle diameter, kinematic viscosity, square of the Hartmann number, dimensionless freestream velocity, particle to fluid viscosity ratio, respectively. It should be mentioned that if M and β are formally equated to zero in Eqs. (9)–(14), the continuity and momentum equations reported by Apazidis [9] will be recovered except the factor 9/2 which is mistakenly missing from his equations.

As explained by Apazidis [8], one of the possible ways that the vertical sedimentation of solid particles may proceed is when a direct shock from the initial particle concentration value to the final fully settled concentration is formed at the interface of a mixture and maximally concentrated dispersed phase settled at the horizontal solid surface. Since this case is quite common and is easier to analyze than the other possible ways in which the particle concentration is non-uniform, it is considered in this work and the volume fraction of particles in the mixture is assumed constant. With this, Eqs. (9) and (12) give

$$\frac{\partial V}{\partial\eta}=\frac{\partial V_p}{\partial\eta}=0 \tag{16}$$

Also, with the assumption of zero volumetric flux in the vertical direction as in the case of batch sedimentation (Wallis [16]), one may write

$$\alpha V_p+(1-\alpha)V=0 \tag{17}$$

Furthermore, assuming that the vertical motion of both phases due to the gravity field has reached its stationary state ($\partial V_p/\partial\tau=\partial V/\partial\tau=0$) and using Eqs. (11), (14), and (17) result in the following vertical components of the velocity fields of both phases:

$$V=\frac{2}{9}\frac{\alpha^2(1-\alpha)}{f(\alpha)},\quad V_p=-\frac{2}{9}\frac{\alpha(1-\alpha)^2}{f(\alpha)} \tag{18}$$

The interface vertical velocity can be shown to be

$$V_i=\frac{2}{9}\frac{\alpha^2(1-\alpha)^2}{(\alpha_M-\alpha)f(\alpha)} \tag{19}$$

where α_M (≈0.6 for spherical particles) is the volume fraction of particles in the dense sediment near the surface (see Apazidis [8]).

The x-momentum equations (10) and (13) governing the horizontal velocity distributions of both phases (U and U_p) can be transformed by using a new coordinate system which moves upwards with the interface velocity V_i such that

$$\eta^*=\eta-V_i\tau \tag{20}$$

to yield

$$\mathrm{Re}\left[\frac{\partial U}{\partial \tau}+(V-V_i)\frac{\partial U}{\partial \eta^*}\right]=\frac{\partial^2 U}{\partial \eta^{*2}}-\frac{9}{2}\frac{f(\alpha)}{(1-\alpha)}(U-U_p)-M^2(U-U_\infty) \tag{21}$$

$$\gamma\,\mathrm{Re}\left[\frac{\partial U_p}{\partial \tau}+(V_p-V_i)\frac{\partial U_p}{\partial \eta^*}\right]=\beta\frac{\partial^2 U_p}{\partial \eta^{*2}}+\frac{9}{2}\frac{f(\alpha)}{\alpha}(U-U_p) \tag{22}$$

Analytical Results

Analytical solutions for the particulate suspension flow behavior of the problem under consideration are obtained for two physical cases. The first case is that of steady hydromagnetic two-phase flow over an infinite surface while the second case deals with hydromagnetic two-phase flow due to an oscillating infinite surface.

Case 1: Steady Hydromagnetic Two-Phase Flow Over an Infinite Surface. For this case the x-momentum equations of both phases (21) and (22) (with the asterisks being dropped) and the appropriate boundary conditions can be written as

$$\mathrm{Re}\left[(V-V_i)\frac{dU}{d\eta}\right]=\frac{d^2U}{d\eta^2}-\frac{9}{2}\frac{f(\alpha)}{(1-\alpha)}(U-U_p)-M^2(U-U_\infty) \tag{23}$$

$$\gamma\,\mathrm{Re}\left[(V_p-V_i)\frac{dU_p}{d\eta}\right]=\beta\frac{d^2U_p}{d\eta^2}+\frac{9}{2}\frac{f(\alpha)}{\alpha}(U-U_p) \tag{24}$$

$$\eta=0:\quad U=0, \tag{25a}$$

$$U_p=S\frac{dU_p}{d\eta} \tag{25b}$$

$$\eta=\infty:\quad U=U_\infty, \tag{25c}$$

$$U_p=U_\infty \tag{25d}$$

where S is a dimensionless wall particulate slip factor. It should be noted that while the exact boundary condition to be satisfied by a particle phase at a surface is not well understood at present, the form used in Eq. (25b) is borrowed from rarefied gas dynamics and has been used by several previous authors (see, for instance, Soo [21] and Chamkha [22]).

Equations (23) and (24) can be combined into a fourth-order ordinary differential equation in terms of U_p. This is done by solving for U from Eq. (24) and then substituting the result into Eq. (23) to yield

$$\beta\Gamma_1\frac{d^4U_p}{d\eta^4}-\Gamma_1[\mathrm{Re}(V-V_i)\beta+\Gamma_2]\frac{d^3U_p}{d\eta^3}-[1-\Gamma_1\Gamma_2\,\mathrm{Re}(V-V_i)+\beta(\Delta+M^2\Gamma_1)]\frac{d^2U_p}{d\eta^2}+[\mathrm{Re}(V-V_i)+\Gamma_2(\Delta+M_2\Gamma_1)]\frac{dU_p}{d\eta}+M^2U_p=M^2U_\infty \tag{26}$$

where

$$\Gamma_1=\frac{2}{9}\frac{\alpha}{f(\alpha)},\quad \Gamma_2=\gamma\,\mathrm{Re}(V_p-V_i),\quad \Delta=\frac{\alpha}{1-\alpha} \tag{27}$$

Inviscid Particle Phase (β=0). For this situation, Eq. (26) reduces to

$$N_1\frac{d^3U_p}{d\eta^3}+N_2\frac{d^2U_p}{d\eta^2}+N_3\frac{dU_p}{d\eta}+N_4U_p=-N_4U_\infty \tag{28}$$

where

$$N_1=\Gamma_1\Gamma_2,\quad N_2=1-\Gamma_1\Gamma_2\,\mathrm{Re}(V-V_i)$$
$$N_3=\mathrm{Re}(V_i-V)-\Gamma_2(\Delta+M^2\Gamma_1),\quad N_4=-M^2 \tag{29}$$

Three boundary conditions are needed to solve Eq. (28). These are given by Eqs. (25a,c,d). Equation (25b) is ignored since for β=0, the particle-phase momentum equation becomes a first-order differential equation and only one boundary condition (25d) is needed.

Without going into detail, it can be shown that the general solution of Eq. (28) subject to the boundary conditions can be written as

$$U_p=U_\infty\left[1-\frac{1}{(1-\Gamma_1\Gamma_2\lambda_1)}\exp(-\lambda_1\eta)\right] \tag{30}$$

where λ_1 is the absolute value of the only negative real root of the characteristic equation:

$$N_1\lambda^3+N_2\lambda^2+N_3\lambda+N_4=0 \tag{31}$$

With the solution of U_p being known, Eqs. (23) or (24) can be solved for U to give

$$U=U_\infty[1-\exp(-\lambda_1\eta)] \tag{32}$$

It should be mentioned that the physical solution of Eq. (28) requires that the characteristic equation (31) has two positive real roots and one negative real root. More than one negative root makes the problem to be underdetermined. While there is no analytical method to show the existence of two positive and one negative roots for Eq. (31), this condition was satisfied in all the results obtained for this case. It can be shown that as $M\to 0$ in Eqs. (30) and (32), the solutions of Apazidis [8] are recovered provided that his parameters are related properly to those of the present work. It is an interesting fact that the form of the solution for a nonzero magnetic field is the same as that without a magnetic field. The effects of the magnetic field are all contained in changes of the real characteristic root λ_1.

Figure 1 presents the effects of the Hartmann number M, the particle Reynolds number Re and the particle-phase volume fraction α on the fluid-phase displacement thickness of the viscous layer $1/\lambda_1$ for a density ratio γ=1000. It is observed that increases in the values of Re causes the viscous boundary layer close to the surface to decrease as a result of convection of momentum toward the interface between the particulate suspension and the layer of sediment at the bottom. Application of a magnetic field normal to the flow direction for the problem considered gives rise to a motive force acting in the flow direction which tends to aid the flow along the horizontal surface. This causes both the fluid- and particle-phase horizontal velocities to increase and their viscous boundary layers to decrease. These behaviors are evident from the decreases in $1/\lambda_1$ as the Hartmann number M increases shown in Fig. 1. From other results not presented herein for brevity, it was observed that the velocity profiles of both phases increase while their displacement thicknesses decrease (see Fig. 1) as the particle-phase volume fraction increases. In addition, these velocities separate in the vicinity of the surface for low values of α and that this separation close to the surface reduces as α increases. This behavior is associated with the fact that, for large density differences between the phases as employed in Fig. 1, the particle-

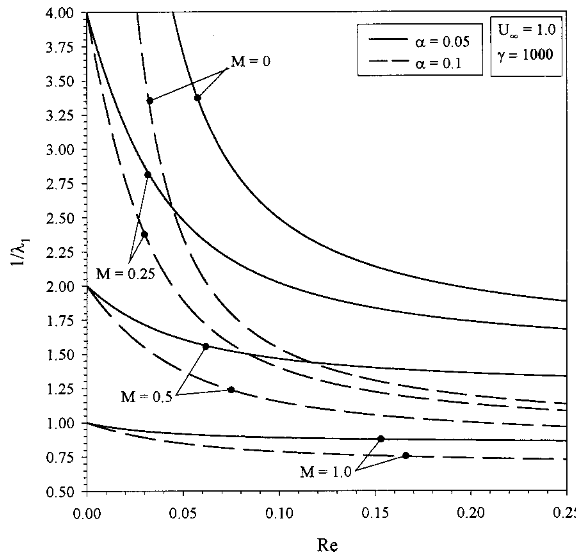

Fig. 1 Effects of *M*, Re, and α on the fluid-phase displacement thickness

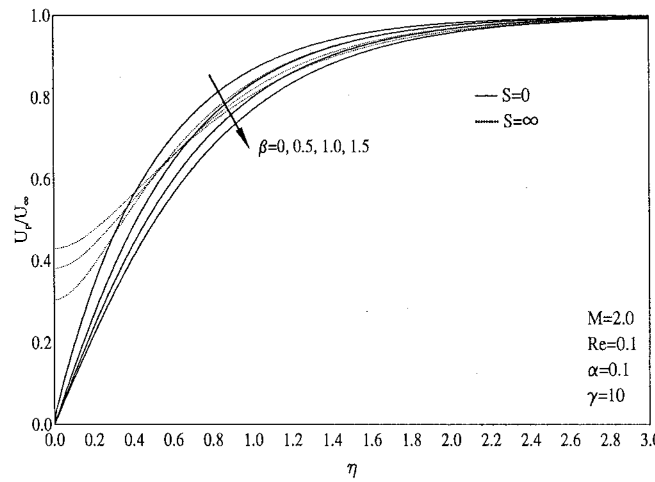

Fig. 3 Effects of *S* and β on particle-phase velocity profiles

phase inertia prevents the adjustment of the horizontal velocity of the particle phase to that of the fluid phase causing a nonzero particle-phase horizontal velocity at the interface.

Figure 2 shows the magnitude of the velocity difference $(U_p - U)$ at $\eta=0$ (or the particle-phase velocity at the interface since the fluid-phase velocity there vanishes due to the no-slip condition) versus Re and for various values of M and γ. It is observed that, for the parametric conditions used, the interface velocity difference increases as Re increases. This is associated with the increase in the velocities of both phases as Re increases mentioned above. Also, the velocity difference at $\eta=0$ is predicted to be lower for $\gamma=100$ than for $\gamma=1000$ as explained above. The effect of the magnetic field is seen to increase the velocity difference at the interface.

Viscous Particle Phase ($\beta\neq 0$). For this particular case, Eq. (26) has the following characteristic equation:

$$N_{11}s^4+N_{22}s^3+N_{33}s^2+N_{44}s+N_{55}=0 \tag{33}$$

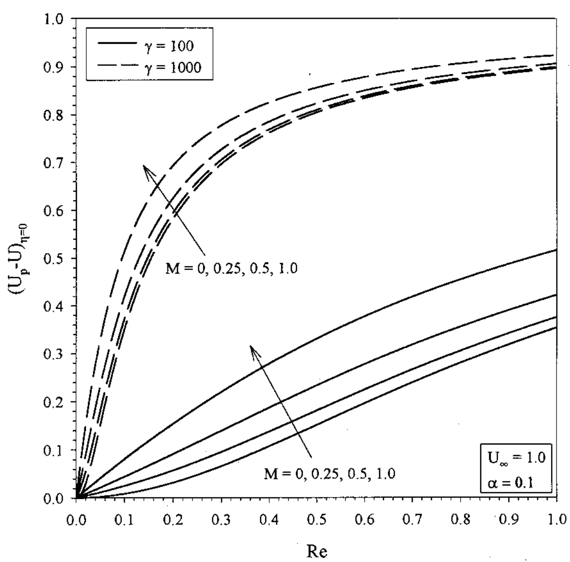

Fig. 2 Effects of *M*, Re, and γ on the velocity difference at the interface

where

$$N_{11}=\beta\Gamma_1,\quad N_{22}=-\mathrm{Re}(V-V_i)\Gamma_1\beta-\Gamma_1\Gamma_2$$
$$N_{33}=-1+\Gamma_1\Gamma_2\,\mathrm{Re}(V-V_i)-\beta(\Delta+M^2\Gamma_1) \tag{34}$$
$$N_{44}=\mathrm{Re}(V-V_i)+\Gamma_2(\Delta+M^2\Gamma_1),\quad N_{55}=M^2$$

The physical solution of Eq. (33) requires that it has two negative and two positive real roots. Without going into detail, the general solutions for U_p and U can be written as

$$U_p=U_\infty+C_1\exp(-s_1\eta)+C_2\exp(-s_2\eta) \tag{35}$$

$$U=U_\infty+C_1M_1\exp(-s_1\eta)+C_2M_2\exp(-s_2\eta) \tag{36}$$

where C_1 and C_2 are arbitrary constants, s_1 and s_2 are the absolute values of the two negative roots of Eq. (33) and

$$M_1=1-\Gamma_1\beta s_1^2-\Gamma_1\Gamma_2 s_1,\quad M_2=1-\Gamma_1\beta s_2^2-\Gamma_1\Gamma_2 s_2 \tag{37}$$

The constants C_1 and C_2 are determined by application of the boundary conditions (25) and can be shown to be

$$C_1=\frac{U_\infty(x_2-M_2)}{(x_1M_2-x_2M_1)};\quad C_2=\frac{U_\infty(x_1-M_1)}{(x_2M_1-x_1M_2)}; \tag{38}$$

where

$$x_1=1+Ss_1,\quad x_2=1+Ss_2 \tag{39}$$

Figure 3 displays the influence of the viscosity ratio β on the particle-phase horizontal velocity U_p for the two cases of no particle wall slip $(S=0)$ and perfect particulate wall slip $(S=\infty)$. For the case of no slip $(S=0)$, it is apparent that the velocity component U_p is zero at the interface between the mixture and the sediment layer as it should be. On the other hand, U_p is nonzero for the case where the particles undergo perfect slip at the interface. The presence of a particle-phase viscosity in the model causes increases in the effective viscosity of the mixture. This, in turn, produces retardation in the motion of the particle phase. This slower motion of the particle phase causes the fluid phase to move slower as well because of the interphase drag force between the fluid and the particle phases. Thus, further increases in the particle-phase viscosity produce further decreases in the motions of both the fluid and the particle phases for the case of no particulate wall slip. However, for the case of perfect particulate wall slip, the reductions in the particle-phase horizontal velocity due to increases in the particle-phase viscosity occur everywhere above the surface except in the immediate vicinity of the interface where the particle-phase horizontal velocity tends to increase as β increases. These behaviors are evident from Fig. 3.

Case 2: Hydromagnetic Two-Phase Flow due to an Oscillating Infinite Surface. For this case the fluid-phase wall velocity has the dimensionless form

$$U = U_0 \cos(\omega\tau) \tag{40}$$

where U_0 and ω are the amplitude and the frequency of wall velocity oscillation.

It should be noted here that the layer of sediment settling on the surface is assumed to be stationary with respect to its horizontal motion. Therefore, it performs harmonic oscillations in the horizontal direction as that of the surface. Far from the surface, the flow is at rest. This is represented by

$$U(\tau,\infty) = U_p(\tau,\infty) = 0 \tag{41}$$

The general unsteady equations (21) and (22) are solved subject to Eqs. (40) and (41) for $U(\tau,\eta)$ and $U_p(\tau,\eta)$ by assuming

$$U(\tau,\eta) = U_0 \cos(\omega\tau + \delta\eta)\exp(-m\eta) \tag{42}$$

$$U_p(\tau,\eta) = [D_1 \cos(\omega\tau + \delta\eta) + D_2 \sin(\omega\tau + \delta\eta)]\exp(-m\eta) \tag{43}$$

where δ, D_1, D_2, and m are constants which make Eqs. (21) and (22) subject to Eqs. (40) and (41) identically satisfied by the solutions (42) and (43). It should be noted that these solutions represent two damped transverse waves propagating into the mixture's interior. The depth of penetration of these waves is dependent on both the wave velocity and wavelength which are functions of the particle Reynolds number Re, particle volume fraction α, density ratio γ, frequency of oscillations ω, Hartmann number M, and the viscosity ratio β. This is in direct contrast with the single-phase flow case for which the depth of penetration is only a function of the fluid viscosity and the frequency of surface oscillations. These behaviors will be shown in the graphical results for this case. Also, it is understood that the particle-phase velocity solution given by Eq. (43) applies for both cases of inviscid and viscous particle phase and that the particle-phase wall condition (25*b*) is not imposed.

Substitution of Eqs. (42) and (43) into Eqs. (21) and (22) results in two equations of the general form:

$$P_1 \cos(\omega\tau + \beta\eta) + P_2 \sin(\omega\tau + \beta\eta) = 0 \tag{44}$$

where P_1 and P_2 are functions of the constants δ, D_1, D_2, and m. Equating P_1 and P_2 of each of the obtained two equations to zero results in the following system of equations:

$$\mathrm{Re}(V - V_i)m + m^2 - \delta^2 - \frac{9}{2}\frac{f(\alpha)}{(1-\alpha)}\left(1 - \frac{D_1}{U_0}\right) - M^2 = 0 \tag{45}$$

$$\mathrm{Re}\,\omega + \mathrm{Re}(V - V_i)\delta + 2m\delta + \frac{9}{2}\frac{f(\alpha)}{(1-\alpha)}\frac{D_2}{U_0} = 0 \tag{46}$$

$$\gamma\,\mathrm{Re}[mD_1 - D_2\omega - (V_p - V_i)D_2\delta] - \beta D_1\delta^2 - 2mD_2\delta\beta + \beta m^2 D_1 + \frac{9}{2}\frac{f(\alpha)}{\alpha}(U_0 - D_1) = 0 \tag{47}$$

$$\gamma\,\mathrm{Re}[D_1\omega + mD_2 + (V_p - V_i)D_1\delta] - \beta D_2\delta^2 + 2mD_1\delta\beta + \beta m^2 D_2 - \frac{9}{2}\frac{f(\alpha)}{\alpha}D_2 = 0 \tag{48}$$

Equations (45)–(48) represent four nonlinear algebraic equations with four unknowns (δ, D_1, D_2, and m) which must be solved numerically. For fast convergence of the solutions, the following procedure is followed. First, Eqs. (45) and (46) are solved for D_1 and D_2 in terms of δ and m, respectively. Second, the obtained expressions for D_1 and D_2 are then substituted into Eq. (48) which produces a quadratic equation in m with the coefficients containing the constant δ. For an assumed value of δ and given values of the involved physical parameters, the roots of this quadratic equation which are real and of opposite signs can be obtained. Therefore, the negative root is chosen and its absolute value is the needed value of m. With the value of m being known for the assumed δ, the constants D_1 and D_2 can then be determined from Eqs. (45) and (46) as mentioned above. Finally, the values of m, D_1, and D_2 are substituted into Eq. (47) which is then solved for δ. As long as $\delta_{\text{assumed}} \neq \delta_{\text{obtained}}$, the same iteration procedure continues until convergence is achieved within a prescribed acceptable error.

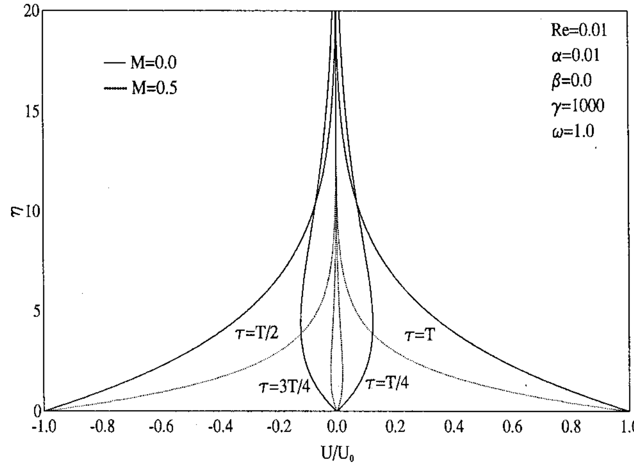

Fig. 4 Effects of *M* on fluid-phase periodic velocity distribution

Results based on the solutions of U and U_p given by Eqs. (42) and (43) are displayed in Figs. 4–6 to illustrate the influence of the Hartmann number M and the viscosity ratio β.

Figures 4 and 5 display the effects of the Hartmann number M on the fluid- and particle-phase periodic horizontal velocity distributions in air-particle flow for $\mathrm{Re}=0.01$, $\alpha=0.01$, $\beta=0$ and $\omega=1.0$, respectively. As in the case of a stationary wall, the effect of the magnetic field increases both the fluid- and particle-phase horizontal velocities (for $\tau = T/2$ and $\tau = 3T/4$) while it produces lower horizontal velocity distributions for both phases (for $\tau = T$ and $\tau = T/4$). It is also observed from these figures that the magnetic field effect speeds up the approach of both phases to the free stream hydrodynamic conditions existing far above the surface.

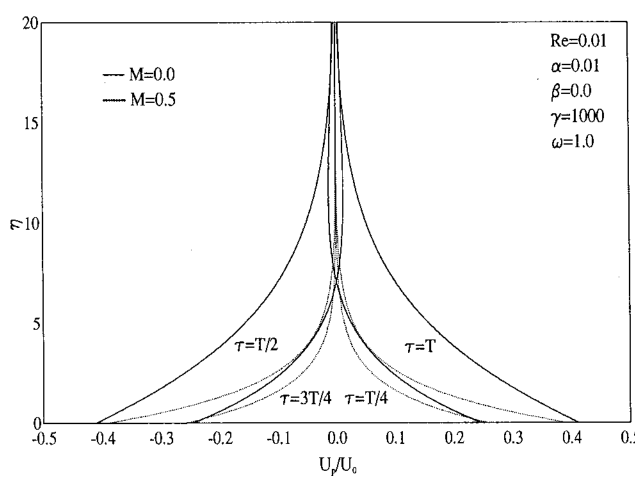

Fig. 5 Effects of *M* on particle-phase periodic velocity distribution

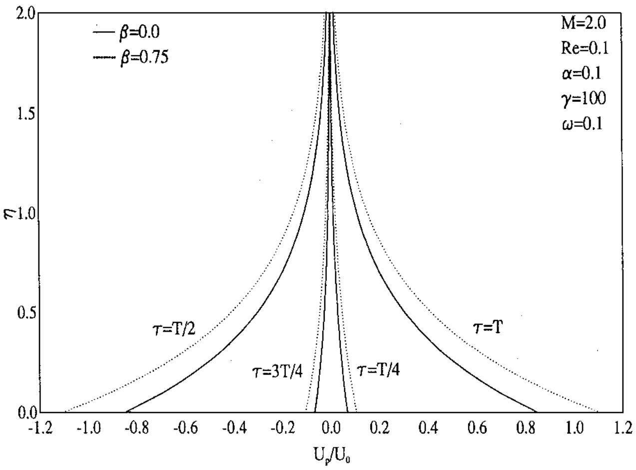

Fig. 6 Effects of β on particle-phase periodic velocity distribution

Figure 6 displays the effects of the viscosity ratio β on the particle-phase horizontal velocity component U_p/U_0. It is predicted that U_p/U_0 increases for $\tau=T$ and $\tau=T/4$ and decreases for $\tau=T/2$ and $\tau=3T/4$ due to increases in the values of β and that the wall velocity exceeds that of the amplitude of oscillations of the surface. The effect of β on the fluid-phase horizontal velocity component U/U_0 for this case was found to be insignificant. Again, it should be noted that in the absence of the magnetic field ($M=0$) and the viscosity ratio ($\beta=0$), the results of Apazidis [8] for the problem of two-phase flow due to an oscillating infinite surface are obtained provided that his parameters are properly related to those reported in this work.

Skin-Friction Coefficients. Of special interest for this problem are skin-friction coefficients of both phases. The shear stresses for the fluid and the particle phases at the interface between the particulate suspension and the layer of sediment on the surface can be defined, respectively, as follows:

$$\tau_f=(1-\alpha)\mu\frac{\partial u}{\partial y}\bigg|_{y=0}=(1-\alpha)\frac{\mu g a\gamma}{\nu}\frac{\partial U}{\partial \eta}\bigg|_{\eta=0},$$

$$\tau_p=\alpha\mu_p\frac{\partial u_p}{\partial y}\bigg|_{y=0}=\alpha\frac{\mu_p g a\gamma}{\nu}\frac{\partial U_p}{\partial \eta}\bigg|_{\eta=0} \quad (49)$$

The dimensionless skin-friction coefficients for both the fluid and the particle phases can be written, respectively, as

$$C_f=\frac{\tau_f}{\rho g a\gamma}=(1-\alpha)\frac{\partial U}{\partial \eta}\bigg|_{\eta=0},\quad C_p=\frac{\tau_p}{\rho g a\gamma}=\alpha\beta\frac{\partial U_p}{\partial \eta}\bigg|_{\eta=0} \quad (50)$$

For the case of steady hydromagnetic two-phase flow over an infinite surface, Eqs. (50) take on the respective forms:

$$C_f=(1-\alpha)U_\infty\lambda_1,\quad C_p=0 \quad (51)$$

for the inviscid particle phase case, and

$$C_f=-(1-\alpha)(C_1s_1M_1+C_2s_2M_2),\quad C_p=-\alpha\beta(C_1s_1+C_2s_2) \quad (52)$$

for the viscous particle phase case.

Figure 7 illustrates the influence of the parameters M, α, and Re on the complete skin-friction coefficient (C_f+C_p) at the interface between the fluid-particle mixture and the sediment layer on the surface for the case of a viscous particle phase ($\beta\neq 0$). Inspection of Fig. 1 shows that both the fluid-phase viscous boundary layer close to the interface and that of the particle phase decrease causing the wall slopes of the fluid- and particle-phase horizontal velocity profiles to increase as either of M, α, or Re increases. This has the direct effect of increasing the complete skin-friction coefficient as shown in Fig. 7.

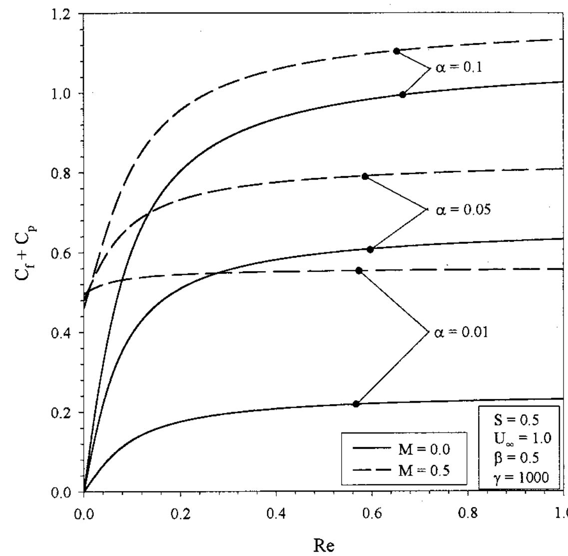

Fig. 7 Effects of M, Re and α on the complete skin-friction coefficient

Figure 8 depicts the influence of all of the density ratio γ, viscosity ratio β, and the particulate wall slip parameter S on the complete skin-friction coefficient (C_f+C_p). In general, individual results for C_f and C_p which are not presented herein show that they increase with increasing values of γ and that the values of C_f decrease while the values of C_p increase with increasing values of β resulting in a net increase in the complete skin-friction coefficient. The increase in the values of C_p as β increases is related to the definition of C_p as being directly proportional to β. Also, in this figure, two situations of no particulate wall slip ($S=0$) and some particulate wall slip ($S=0.5$) are shown. It is predicted that as S increases, the wall slope of the fluid-phase velocity increases while that of the particle phase decreases caus-

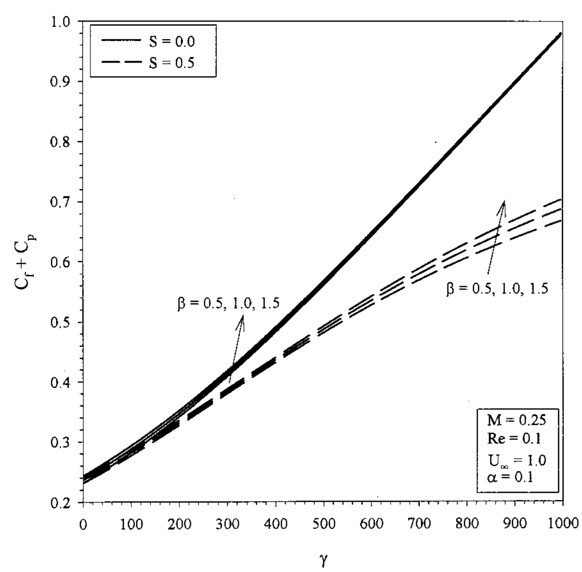

Fig. 8 Effects of S, β and γ on the complete skin-friction coefficient

ing respective increases and decreases in the values of C_f and C_p. As a result, the complete skin-friction coefficient is lower for $S=0.5$ than that for $S=0$.

Conclusion

This work was focused on the problem of hydromagnetic particulate suspension flow over a horizontal impermeable surface in the presence of a gravity field. The particle phase was assumed to be somewhat dense and, as a consequence, it was endowed by an artificial viscosity. A boundary condition borrowed from rarefied gas dynamics allowing for general situations of particulate wall slip conditions was employed. Analytical solutions for the velocity distributions and the skin-friction coefficients of both phases were obtained for stationary and periodic wall velocity conditions. Representative results for various parametric conditions were presented graphically to elucidate interesting features of the solutions. It was found that the presence of a magnetic field increased the motion of the mixture along the surface with increased values in the fluid-phase skin-friction coefficient. On the other hand, while the presence of a particle-phase viscosity increased the skin-friction coefficient for the particle phase, it produced reductions in the fluid-phase skin-friction coefficient. Allowing the particle phase to undergo a certain amount of slip at the interface between the layer of sediment and the mixture caused increases in the fluid-phase skin-friction coefficient and decreases in the particle-phase skin-friction coefficient. It is hoped that the present work be used as a vehicle for understanding other particle-phase stress models and other body force effects.

Nomenclature

a = particle radius
B_0 = magnetic induction
C_f = fluid-phase skin-friction coefficient ($C_f=(1-\alpha)\partial U/\partial\eta|_{\eta=0}$)
C_p = particle-phase skin-friction coefficient ($C_p=\alpha\beta\partial U_p/\partial\eta|_{\eta=0}$)
f = correction factor defined by Eq. (7)
g = gravitational acceleration
M = Hartmann number ($M^2=\sigma B_0^2 a^2/\mu$)
p = fluid-phase pressure
P = dimensionless fluid-phase reduced pressure
Re = particle Reynolds number ($\mathrm{Re}=ga^3\gamma/\nu^2$)
S = dimensionless particle-phase wall slip factor
t = time
u = fluid-phase x-component of velocity
U = dimensionless fluid-phase horizontal velocity ($U=\nu/(ga^2\gamma)u$)
v = fluid-phase y-component of velocity
V = dimensionless fluid-phase normal velocity ($V=\nu/(ga^2\gamma)v$)
x = distance along the surface
y = distance normal to the surface

Greek Symbols

α = volume fraction of particles
β = particle-to-fluid viscosity ratio ($\beta=\mu_p/\mu$)
α_m = dense sediment particulate volume fraction ($\alpha_m\simeq 0.6$)
η = dimensionless vertical distance ($\eta=y/a$)
γ = particle-to-fluid density ratio ($\gamma=\rho_p/\rho$)
μ = fluid-phase dynamic viscosity
ν = fluid-phase kinematic viscosity
ω = frequency of oscillation of wall velocity
ρ = fluid-phase density
σ = fluid-phase electrical conductivity
τ = dimensionless time ($\tau=ga\gamma/\nu t$)
τ_f = fluid-phase shear stress at the interface defined by Eqs. (49)
τ_p = particle-phase shear stress at the interface defined by Eqs. (49)

Subscripts

i = interface
p = particle phase
∞ = free stream

References

[1] Yiantsios, S. G., and Karabelas, A. J., 1998, ''The effect of gravity on the deposition of micron-sized particles on smooth surfaces,'' Int. J. Multiphase Flow, **24**, pp. 283–293.
[2] Jia, X., and Williams, R. A., 1990, ''Particle/deposition at a charged solid/liquid interface,'' Chem. Eng. Commun., **91**, pp. 127–198.
[3] Ven van de, T. G. M., 1989, *Colloidal Hydrodynamics*, Academic Press, London.
[4] Yao, K. M., Habibian, M. T., and O'Melia, C. R., 1971, ''Water and waste water filtration: concepts and applications,'' Environ. Sci. Technol., **5**, pp. 1105–1112.
[5] Adamczyk, Z., and van de Ven, T. G. M., 1981, ''Deposition of particles under external forces in laminar flow through parallel-plate and cylindrical channels,'' J. Colloid Sci., **80**, pp. 340–356.
[6] Adamczyk, Z., and van de Ven, T. G. M., 1982, ''Particle transfer to a plate in uniform flow,'' Chem. Eng. Sci., **37**, pp. 869–880.
[7] Marmur, A., and Ruckenstein, E., 1986, ''Gravity and cell adhesion,'' J. Colloid Interface Sci., **114**, pp. 261–266.
[8] Apazidis, N., 1985, ''On two-dimensional laminar flows of a particulate suspension in the presence of a gravity field,'' Int. J. Multiphase Flow, **11**, pp. 657–698.
[9] Apazidis, N., 1990, ''Temperature distribution and heat transfer in a particle-fluid flow past a heated horizontal plate,'' Int. J. Multiphase Flow, **16**, pp. 495–513.
[10] Dahlkild, A. A., 1997, ''The motion of Brownian particles and sediment on an inclined plate,'' J. Fluid Mech., **337**, pp. 25–47.
[11] Chen, C. P., and Wood, P. E., 1986, ''Turbulence closure modeling of the dilute gas-particle axisymmetric jet,'' AIChE J., **32**, pp. 163–166.
[12] Drew, D. A., and Segal, L. A., 1971, ''Analysis of fluidized beds and foams using averaged equations,'' Stud. Appl. Math., **50**, pp. 233–252.
[13] Gidaspow, D., 1986, ''Hydrodynamics of fluidization and heat transfer: super computer modelling,'' Appl. Mech. Rev., **39**, pp. 1–23.
[14] Tsuo, Y. P., and Gidaspow, D., 1990, ''Computation of flow patterns in circulating fluidized beds,'' AIChE J., **36**, pp. 888–896.
[15] Gadiraju, M., Peddieson, J., and Munukutla, S., 1992, ''Exact solutions for two-phase vertical pipe flow,'' Mech. Res. Commun., **19**, pp. 7–13.
[16] Wallis, G. B., 1969, *One-dimensional Two-phase Flow*, McGraw-Hill, New York.
[17] Kynch, G. J., 1952, ''A theory of sedimentation,'' Trans. Faraday Soc., **48**, pp. 166–176.
[18] Cramer, K. R., and Pai, S.-I., 1973, *Magnetofluid Dynamics for Engineers and Applied Physicists*, Scripta Publishing Company, Washington, D.C.
[19] Marble, F. E., 1970, ''Dynamic of dusty gases,'' Annu. Rev. Fluid Mech., **2**, pp. 397–446.
[20] Tam, K. W., 1969, ''The drag on a cloud of spherical particles in low Reynolds number flow,'' J. Fluid Mech., **38**, pp. 537–546.
[21] Soo, S. L., 1989, *Particulates and Continuum Multiphase Fluid Dynamics*, Hemisphere Publishing, New York, pp. 282 and 292.
[22] Chamkha, A. J., 1996, ''Compressible dusty-gas boundary-layer flow over a flat surface,'' ASME J. Fluids Eng., **118**, pp. 179–185.